JOURNAL OF GEOPHYSICAL RESEARCH, VOL. 112, D10109, doi:10.1029/2006JD007631, 2007



# Are lightning M components capable of initiating sprites and sprite halos?

S. A. Yashunin,[1] E. A. Mareev,[1] and V. A. Rakov[2]

Received 7 June 2006; revised 8 December 2006; accepted 14 December 2006; published 19 May 2007.

[1] The role of the M component mode of charge transfer to ground in lightning discharges in initiating sprites and sprite halos is examined. M components (surges superimposed on lightning continuing currents) serve to enhance the electric field at high altitudes and, as a result, may increase the probability of sprite (halo) initiation. It appears that occurrence of an M component shifts electric field maximum from the axis of the vertical lightning channel and therefore increases the likelihood of initiation of sprites displaced from the channel axis. Since M components follow return strokes after a time interval of a few milliseconds or more, they may be primary producers of so-called delayed sprites.

**Citation:** Yashunin, S. A., E. A. Mareev, and V. A. Rakov (2007), Are lightning M components capable of initiating sprites and sprite halos?, *J. Geophys. Res.*, *112*, D10109, doi:10.1029/2006JD007631.

## 1. Introduction

[2] Lightning M components are transient perturbations in the relatively steady continuing current that follows the return stroke pulse and in the associated channel luminosity [*Rakov and Uman*, 2003]. Best documented and studied M components are associated with negative lightning discharges, in which they serve to transport negative electric charge from cloud to ground. However, positive lightning discharges (that are apparently major sprite producers) also exhibit transient variations in their currents, which are probably manifestations of M component mode of positive charge transfer to ground. It is important to note that positive flashes are usually composed of a single stroke followed by a relatively high-magnitude continuing current. Our knowledge of physical properties and statistics of positive lightning is still much poorer than that of negative lightning. However, available data suggest that M components are likely to be common in positive lightning (M. Saba, personal communication, 2006) and that the M component peak current in positive lightning can be much higher (in the tens of kiloamperes range) than the typical values (up to a few kiloamperes) observed in negative lightning [*Rakov and Uman*, 2003]. Indeed, the 20-kA or so pulse at about 3 ms in Figure 1 (top) of *Rakov* [2003] that shows directly measured current in a positive lightning discharge is probably an M component. Further, *Rakov* [2003, Figure 2b] suggested that millisecond-scale positive current waveforms, whose peaks are in the tens to hundreds of kiloamperes range, observed by K. Berger are likely to be a result of M component mode of charge transfer to ground.

[3] It has been suggested [*Rakov et al.*, 2001] that M components in positive lightning may play a role in the initiation of delayed sprites that occur tens of millisecond after the return stroke [e.g., *Cummer et al.*, 1998; *Reising et al.*, 1999]. In this paper, we will provide support to this claim calculating the electric field from the M component at high altitudes above the cloud. Some researchers suggested that delayed sprites might be produced by steady currents in intracloud discharges following return strokes [*Bell et al.*, 1998] or by "unusually intense continuing currents" moving charges of several hundred coulombs to the ground after the return stroke [*Cummer and Füllekrug*, 2001]. In the latter study, the implication appears to be that the continuing current plays a primary role in sprite production, and that there is no need to invoke M components in order to explain delayed sprites. However, M components apparently always accompany continuing currents [e.g., *Fisher et al.*, 1993; *Campos et al.*, 2007; M. Saba, personal communication, 2006], so that it is difficult to distinguish between the effects of these two lightning processes in interpreting sprite observations. Additionally, we will show that M components can play a significant role in the generation of other transient luminous phenomena in the middle atmosphere, such as sprite halos. We developed a simple procedure that allowed analytical estimation of the electrostatic, induction and radiation electric field perturbations in free space. Using this procedure, we examined the importance of relative contributions from the individual field components to the total electric field of lightning flash during its continuing current stage and the spatial distribution of the total electric field. In order to take into account effects of the conducting atmosphere, we performed numerical field calculations using the night atmosphere conductivity profile.

## 2. Model

[4] We use here a two-wave model of the M component proposed by *Rakov et al.* [1995]. M component is modeled

[1]Laboratory of Geophysical Electrodynamics, Institute of Applied Physics, Russian Academy of Sciences, Nihzny Novgorod, Russia.
[2]Department of Electrical and Computer Engineering, University of Florida, Gainesville, Florida, USA.


0148-0227/07/2006JD007631$09.00

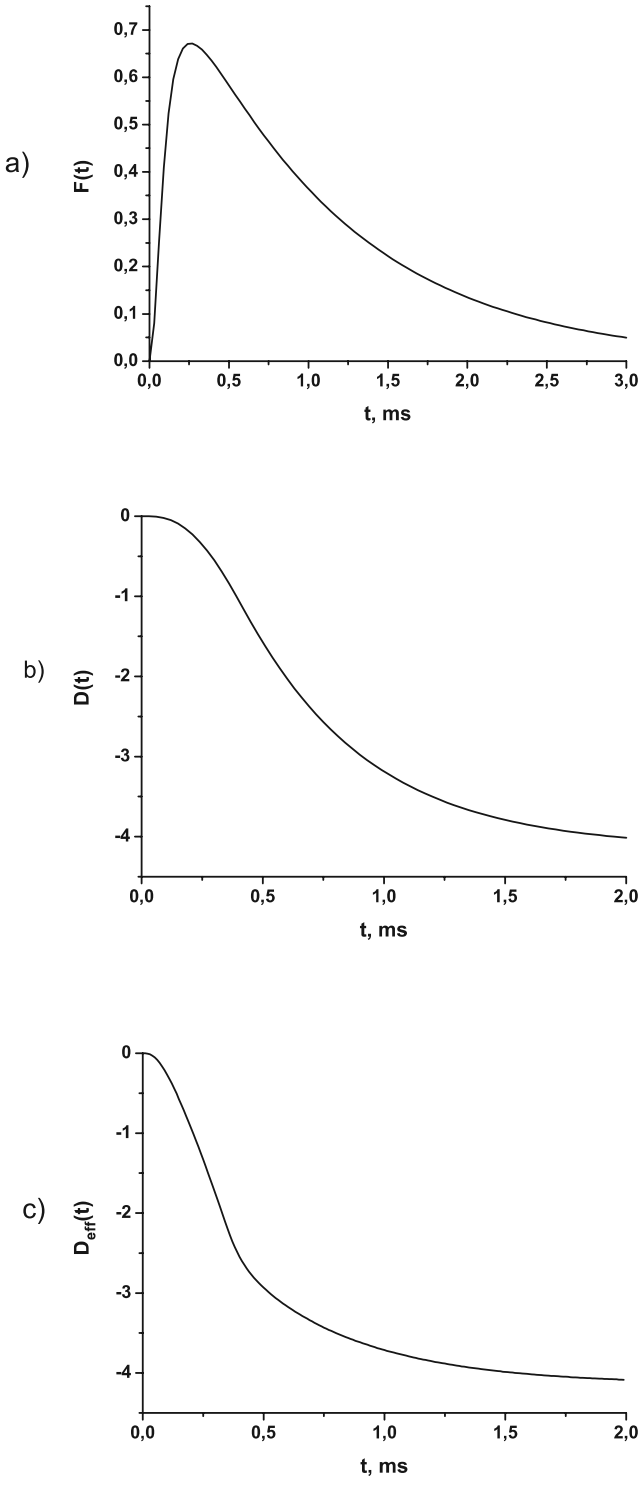


**Figure 1.** Time dependence of dimensionless functions characterizing current dynamics: (a) $F(t)$, (b) $D(t)$, and (c) $D_{\text{eff}}(t)$.

initially as an incident, downward propagating wave and, after the arrival of this wave at ground, as the superposition of the incident wave and a reflected, upward propagating wave. The validity of this model was tested using measurements of the channel base current and associated electric and magnetic fields in the vicinity of the triggered-lightning channel [*Rakov et al.*, 1995, 2001].

[5] We compute the electric field of the lightning M component at mesospheric altitudes. The ground surface is assumed to be a perfect conductor, and lightning channel is assumed to be straight and vertical. The electric field is created by current $I$ and charge $Q$ of the M component, as well as by its image current $I$ and image charge $-Q$. Since the reflection coefficients are equal to $+1$ and $-1$ for the current and for the charge density waves, respectively, the electric field produced by an M component above perfectly conducting ground is equivalent to the field generated by two waves of current and charge density traveling at the same velocity in opposite directions between heights $-h$ and $h$ [*Rakov et al.*, 1995]. The waves are characterized by the same current and by charge densities of the same magnitude but of the opposite polarity.

[6] If the current density is represented by the traveling wave

$$j = \delta(x)\delta(y)I\left(t - \frac{z}{v}\right),$$

the volume charge density can be derived from the charge conservation principle:

$$\rho = \delta(x)\delta(y)\frac{I\left(t - \frac{z}{v}\right)}{v}.$$

Here $v$ is the wave propagation velocity, and $\delta(x)$ and $\delta(y)$ are delta functions. The $z$ axis is directed upward along the lightning channel. For a pair of waves moving vertically in opposite directions one can obtain

$$\begin{aligned}\mathbf{j} &= -\mathbf{z_0}\delta(x)\delta(y)I_z(z,t)\\ &= -\mathbf{z_0}\delta(x)\delta(y)\cdot\left[I\left(t + \frac{z-h}{v}\right) + I\left(t - \frac{z+h}{v}\right)\right] \qquad (1)\end{aligned}$$

$$\rho = \delta(x)\delta(y)\frac{1}{v}\left[I\left(t + \frac{z-h}{v}\right) - I\left(t - \frac{z+h}{v}\right)\right]. \qquad (2)$$

[7] Using expressions (1) and (2), vector and scalar potentials of the electromagnetic field can be written in the form

$$\mathbf{A} = \mathbf{z_0}A_z = -\mathbf{z_0}\frac{1}{4\pi\varepsilon_0 c^2}\int_{-h}^{h}\frac{I\left(t - \frac{R}{c} + \frac{z'-h}{v}\right) + I\left(t - \frac{R}{c} - \frac{z'+h}{v}\right)}{R}dz' \qquad (3)$$

$$\varphi = \frac{1}{4\pi\varepsilon_0 v}\int_{-h}^{h}\frac{I\left(t - \frac{R}{c} + \frac{z'-h}{v}\right) - I\left(t - \frac{R}{c} - \frac{z'+h}{v}\right)}{R}dz', \qquad (4)$$

where $R = |\mathbf{r} - \mathbf{r}'|$. Equations (3) and (4) can be simplified for distances $r \gg h$ (in the following, we assume that $h \leq 10$ km) using the approximation $R = |\mathbf{r} - \mathbf{r}'| \approx r - z'\cos\vartheta$, where $\vartheta$ is the angle between the $z$ axis and vector $\mathbf{r}$. Taking into account inequality $z'\cos\vartheta\, c/ \ll z'/v$ and assuming that

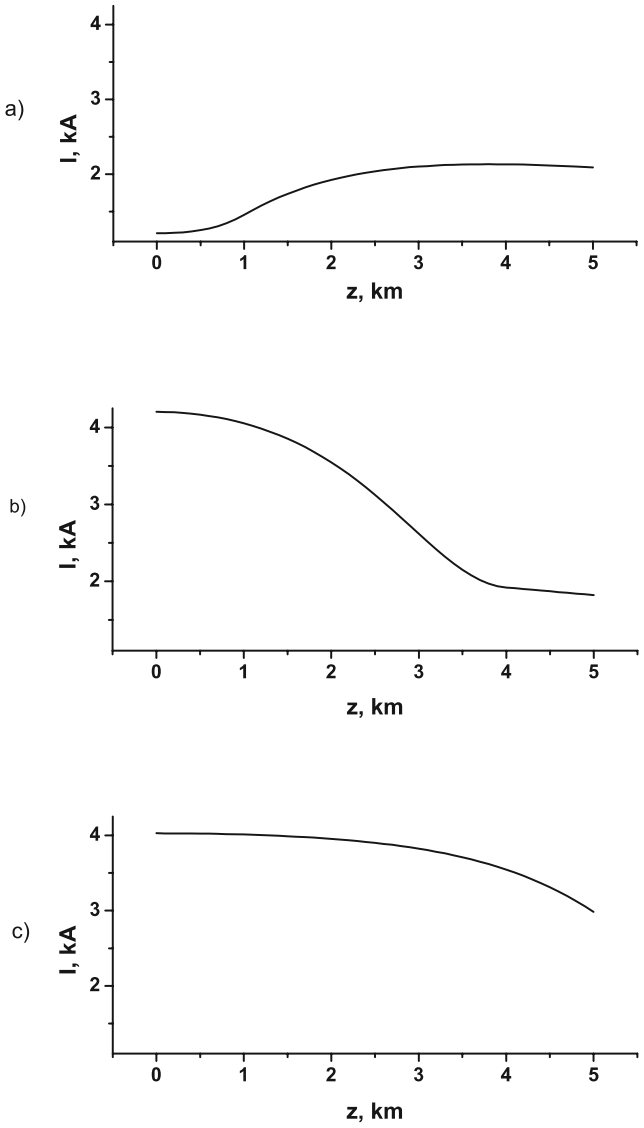


**Figure 2.** M component current distributions along the channel at different times: (a) $t = 0.2$ ms, (b) $t = 0.3$ ms, and (c) $t = 0.5$ ms.

the current varies weakly during the time interval $z' \cos\vartheta / c$, we can rewrite equation (3) for the vector potential as

$$A_z = \frac{1}{4\pi\varepsilon_0 c^2 r} \int_{-h}^{h} I_z(z', t') dz'.$$

[8] Using the charge conservation principle, the last expression can be presented in the form

$$A_z = \frac{\dot{d}_z}{4\pi\varepsilon_0 c^2 r}, \tag{5}$$

where $d_z$ is the vertical component of the dipole moment $\mathbf{d} = \mathbf{z_0} d_z$, evaluated at time $t' = t - r/c$, and $\dot{d}_z$ is the first derivative of $d_z$ with respect to time.

[9] Applying the Lorentz condition, one can express the scalar potential as $\varphi = -div(\mathbf{d}/r)/4\pi\varepsilon_0$ and the electric field as follows:

$$\mathbf{E} = \frac{1}{4\pi\varepsilon_0}\left\{\frac{3(\mathbf{d}\cdot\mathbf{r})\mathbf{r}}{r^5} - \frac{\mathbf{d}}{r^3} + \frac{3(\dot{\mathbf{d}}\cdot\mathbf{r})\mathbf{r}}{cr^4} - \frac{\dot{\mathbf{d}}}{cr^2} + \frac{1}{c^2 r}\left[\left[\ddot{\mathbf{d}}\times\frac{\mathbf{r}}{r}\right]\times\frac{\mathbf{r}}{r}\right]\right\}, \tag{6}$$

where *div* is the divergence operator and $\ddot{\mathbf{d}}$ is the second-order derivative of $\mathbf{d}$ with respect to time. The first two terms in equation (6) correspond to the electrostatic field, the last term describes the radiation field (electromagnetic pulse), and the two intermediate terms the induction field. Equation (6) is convenient for qualitative estimates of the relative importance of individual field component when the relation $\dot{\mathbf{d}} \sim \mathbf{d}/t$ is satisfied with sufficient accuracy. It is clear, in particular, that for long times, $t \gg r/c$ (for $r = 83$ km, for example, $r/c = 276$ $\mu$s), the electrostatic field dominates. On the other hand, for $t \ll r/c$ the radiation field dominates, unless the angle between vectors $\mathbf{d}$ and $\mathbf{r}$ is small. In the latter case, the radiation field vanishes, so that the induction field gives the principal contribution to the total field. *Lu* [2006], who computed electric fields due to return strokes at a height of 90 km, found that the induction field component dominates within a radius of about 11 km (depending on the return stroke speed) of the vertical lightning channel.

[10] Note that the radiation field in equation (6) can be reduced to a simple expression for arbitrary two-wave current density distribution described by equation (1). Indeed, for the second-order derivative of the dipole moment we have

$$\ddot{d}_z = -2v\left[I(t) - I\left(t - \frac{2h}{v}\right)\right]. \tag{7}$$

[11] If the current wave traverses distance $2h$ in time $t$, exceeding the pulse front duration, the maximum value of the second-order derivative is given by $|\ddot{d}_z|_{\max} = 2vI_{\max}$, where $I_{\max}$ is the maximum current of the M component wave.

[12] We will approximate the electric current of the M component as

$$I(0,t) = I_0 F(t) = \begin{cases} I_0 \dfrac{\left(\dfrac{t}{\tau_1}\right)^2 \exp\left(-\dfrac{t}{\tau_2}\right)}{1+\left(\dfrac{t}{\tau_1}\right)^2}, & t > 0 \\ 0, & t \le 0 \end{cases}, \tag{8}$$

where $\tau_1$ is of the order of 100 $\mu$s and $\tau_2$ of the order of 1 ms. The function $F(t)$ for $t > 0$, $\tau_1 = 70$ $\mu$s and $\tau_2 = 0.5$ ms is plotted in Figure 1a. For any given reflection coefficient for current, one can easily find the electric current distribution at an arbitrary time. As an example, current distributions along the lighting channel at $t = 0.2$, 0.3 and 0.5 ms are shown in Figure 2. It is clear that the total current represents the sum of incident and reflected current waves.

[13] When calculating the dipole moment, one should take into account the charges at the points located at $\pm h$ as

well as the charge distributed along the lightning channel, according to equation (2). The point charge at $+h$ is equal in magnitude but opposite in sign to the total charge of the wave originating from this point. The point charge at $-h$ is found in a similar manner. First, consider the wave propagating from $-h$ to $+h$. Then the charge density distribution in the channel as a function of time can be written as $\rho_c = -I_0\, F(t - z/v)/v$, so that the time dependence of the dipole moment for one wave has the form $d(t) = d_z\,(t) = I_0\, D(t)$, where current $I_0$ is expressed in A (amperes), the dipole moment $d(t)$ in C·m, and function $D(t)$ for $2h = 10$ km, $\tau_1 = 70$ $\mu$s and $\tau_2 = 0.5$ ms is plotted in Figure 1b.

[14] Introducing the effective dipole moment, $\mathbf{d}_{eff} = \mathbf{d} + \dot{\mathbf{d}} \cdot r/c$, for one wave of the M component, we can rewrite equation (6) in the form

$$\mathbf{E} = \frac{1}{4\pi\varepsilon_0}\left\{\frac{3(\mathbf{d}_{eff}\cdot\mathbf{r})\mathbf{r}}{r^5} - \frac{\mathbf{d}_{eff}}{r^3} + \frac{1}{c^2 r}\left[\left[\ddot{\mathbf{d}}\times\frac{\mathbf{r}}{r}\right]\times\frac{\mathbf{r}}{r}\right]\right\}, \quad (9)$$

where

$$d_{eff}(t) = d_{eff\ z}(t) = I_0 D_{eff}(t). \quad (10)$$

[15] Function $D_{eff}(t)$ for $2h = 10$ km, $\tau_1 = 70$ $\mu$s, $\tau_2 = 0.5$ ms is plotted in Figure 1c. Note that the effective dipole moment $d_{eff}(t)$ grows faster in time compared to the actual dipole moment $d(t)$, especially at early times. This is caused by the fact that the terms containing the derivative of the dipole moment make the main contribution to the electric field, given by equation (6), at early times. Estimates show that the contribution of the first two terms in equation (9) grows quickly in the time period that is several times less than the M component duration, and then slowly flattens. The last term in equation (9) does not contribute to the field directly above the channel. At late times it vanishes as well. Thus, for late times and small angles with respect to the $z$ axis, the electric field follows the change in the effective dipole moment.

## 3. M Component Electric Field in Free Space

[16] Field perturbation due to an M component can be estimated using equations (6)–(10) for particular parameters of the current. As an example, we consider a lightning stroke with continuing current lasting 15 ms assuming that the continuing current magnitude is constant and equal to 8 kA. In the absence of M component this current transfers a total charge of 120 C, so that for $2h = 10$ km the dipole moment equals $1.2 \times 10^6$ C·m. The peak current of M component is usually several times greater than that of the continuing current. An M component peak current of 18 kA, for instance, corresponds to $I_0 = 30$ kA in equation (8). Then, according to equation (10) and Figure 1 ($\tau_1 = 70$ $\mu$s, $\tau_2 = 0.5$ ms), the total effective dipole moment of M component is $2.5 \times 10^5$ C·m. Its risetime to peak value is 0.4 ms.

[17] It is clear that the M component accelerates the field growth during the continuing current stage. Because the effective ionization rate is a rapidly varying function of the electric field magnitude [*Pasko et al.*, 1997; *Mareev et al.*, 2006], even a small increase in the field is capable of influencing strongly the ionization process, which leads to an increase in the breakdown probability.

[18] Let us explore the dependence of the electric field on angle $\vartheta$ between the $z$ axis and the radius vector $\mathbf{r}$. Let $\mathbf{P}$ be the total dipole moment of the charge distribution during the continuing current stage at the instance of the maximum M component current. For the calculation of the total field we can use equation (9) with $\mathbf{d}_{eff}$ replaced with $\mathbf{P}$. The square of the electric field magnitude can then be written in the form

$$E^2 = \frac{1}{(4\pi\varepsilon_0)^2}\left\{\frac{P^2}{r^6}\left(1+3\cos^2\vartheta\right) + \frac{\ddot{d}^2\sin^2\vartheta}{c^4 r^2} + \frac{2P\ddot{d}\sin^2\vartheta}{c^2 r^4}\right\}. \quad (11)$$

[19] We have taken into account that vectors $\mathbf{P}$ and $\ddot{\mathbf{d}}$ are collinear. To search for the maximum of the field as a function of altitude, we examine $E^2$ as a function of $z$ and $x = \cos^2\vartheta$. It turns out that the field distribution is determined mainly by single dimensionless parameter $a = \frac{z^2\ddot{d}}{Pc^2} > 0$. When $a$ is small, the maximum of the total electric field occurs on the axis of the system ($\vartheta = 0$). We are interested in the case when the electric field has a local maximum at angle $\vartheta > 0$. According to equation (11), this is possible if function $f(x) = 12x^3 + 3x^2\,(1 - 2a) + a^2 + 2xa(2 - a)$ has a root in the interval $x \in [0, 1]$. It is easy to show that such a root exists when $a > 3$. Taking, as the first approximation, $P \approx 2hI\tau$ (that is, assuming that the total moment is dominated by the charge transferred by continuing current), where $I$ is the steady current during the continuing current stage, $\tau$ is the time from the beginning of this stage to the moment when $\ddot{d}$ reaches its maximum, one can write this condition in the form

$$\frac{v}{c}\frac{z^2}{hc\tau}\frac{I}{I_{\max}} > 3. \quad (12)$$

[20] If condition (12) is satisfied, the local maximum of electric field during the M component is attained at some angle $\vartheta$ measured with respect to the $z$ axis. The parameter determining an absolute maximum can be found numerically. To study the behavior of the root of function $f(x)$ for $a > 3$, we assume: $x = 1 - \delta$, $\delta \ll 1$; $a = 3 + \varepsilon$, $\varepsilon \ll 1$, and after simple algebra derive that $\delta^2 = 8\varepsilon/21$, which gives $x = 1 - \sqrt{8\varepsilon/21}$. Expressing $\vartheta$ in terms of $\varepsilon$, we find: $\vartheta = (8\varepsilon/21)^{1/4}$. Therefore angle $\vartheta$ increases quickly at small $\varepsilon$. For example, when $\varepsilon = 0.1$, $\vartheta = 0.44 = 25°$. For large values of parameter $a$ we keep the terms proportional to $a^2$ and find $x = 0.5$, or $\vartheta = 45°$. This means that the angle stops increasing at large values of $a$. Angle $\vartheta$ as a function of $a$ is plotted in Figure 3. It is clear from Figure 3 that the maximum field values of the angle lie primarily between 30° and 45°. Radial distributions of the electric field squared (normalized by the magnitude of the dipole field) at a height of 75 km for different values of parameter $a$ are presented in Figure 4. It follows from Figure 4 that the occurrence of M component leads to the radial expansion of the region occupied by high field during the continuing current stage. Interestingly, recent measurements of transient luminous effects in the middle atmosphere give evidence of rather

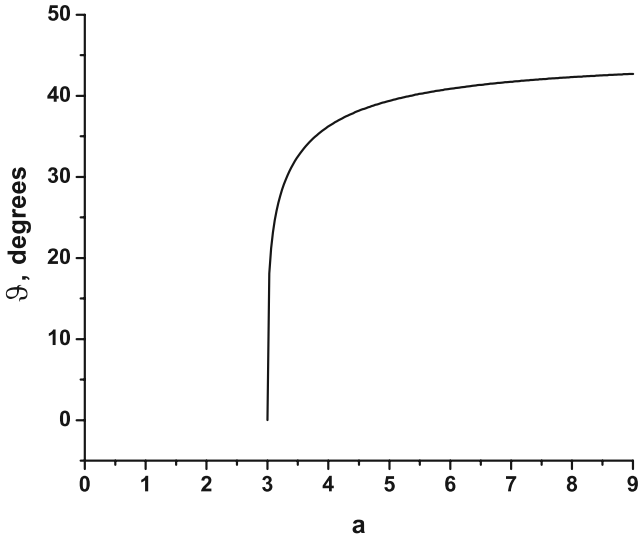


**Figure 3.** Field-maximum angle as a function of parameter *a*.

frequent occurrence of diffuse luminous regions at altitudes 75–85 km with a horizontal extent of 60–70 km, that are referred to as sprite halos [*Barrington-Leigh et al.*, 2001; *Wescott et al.*, 2001; *Bering et al.*, 2004]. Results of our analysis suggest that halo excitation may be related to the electric field of the continuing current that is enhanced by an M component. Further, the electric field generated by an M component should lead to expansion of the luminous region radially because of a rather fast change of the dipole moment.

[21] It was also found [e.g., *Wescott et al.*, 2001; *Füllekrug et al.*, 2001] that sprite structures may occur as far as some tens of kilometers horizontally away from the parent cloud-to-ground flash position, while the point of maximum brightness for sprite halos tends to be centered above the parent lightning discharge. It appears that the electrical breakdown associated with sprites may require a random ionizing (triggering) event. We speculate that, regardless of the nature of this event, the electromagnetic pulse produced by an M component shifts the field maximum from the axis of the vertical lightning channel and therefore increases the probability of sprite triggering at some horizontal distance from the channel axis. Note that a horizontal displacement between the ground strike point (reported, for example, by the NLDN or other similar system) and the effective charge neutralized by lightning (estimated, for example, using a network of field mills) was observed [e.g., *Jacobson and Krider*, 1976] for negative lightning. However, to the best of our knowledge, a similar displacement between channel and charge for positive lightning, which could also explain the lateral displacement between sprites and return stroke channels, has not been reported in the literature.

## 4. Influence of Conductivity of the Atmosphere

[22] We used the following equation [*Mareev et al.*, 2006] in calculating the vertical component of electric field of an M component superimposed on background continuing current with the conductivity of the atmosphere taken into account:

$$\frac{\partial E}{\partial t} + \frac{\sigma(E,z)}{\varepsilon_0} E = \frac{\partial E_{ex}}{\partial t}, \tag{13}$$

where $E_{ex} = \frac{1}{4\pi\varepsilon_0}\frac{P}{z^3}$ is the external dipole field, $P = 2hIt + d_{eff}$ is the full dipole moment, $h$ is the mean height of the region, in which the electric charge transferred by the lightning current is distributed. In the expression for $P$, the first term describes the growth of the dipole moment of the background continuing current, while the second term is the contribution from the perturbation caused by the M component. Application of equation (13) to the continuing current only (without M components) has been justified by *Mareev et al.* [2006] (see also *Pasko et al.* [1997] for comparison). Equation (13) is convenient, because at times that are sufficiently small it gives the dipole field in the vicinity of the source. It should be noted however that it is an approximate equation that ignores the horizontal components of electric field.

[23] It is clear from equation (13) that the conducting medium causes the field relaxation with the characteristic time, $\varepsilon_0/\sigma$ ($E$, $z$), depending on the electric field magnitude. Such a nonlinear effect caused by the collision frequency change due to heating of electrons is pronounced at heights of the lower ionosphere for lightning currents of the order of 1 kA. Focusing on the search for breakdown conditions, we will disregard below the change in conductivity due to electron density perturbation, assuming that near the breakdown threshold the ionization did not have enough time to develop. We used in field calculations a conductivity profile experimentally obtained during night conditions [*Holzworth et al.*, 1985] (see Appendix A for details). The M component velocity is assumed to be equal $0.1c$ ($c$ is the speed of the light in vacuum). The charge source height $h$ is assumed to be 5 km. We assume that the lightning discharge (return stroke followed by continuing current) lasts for 10 ms, and then field relaxation takes place. The charge transferred by

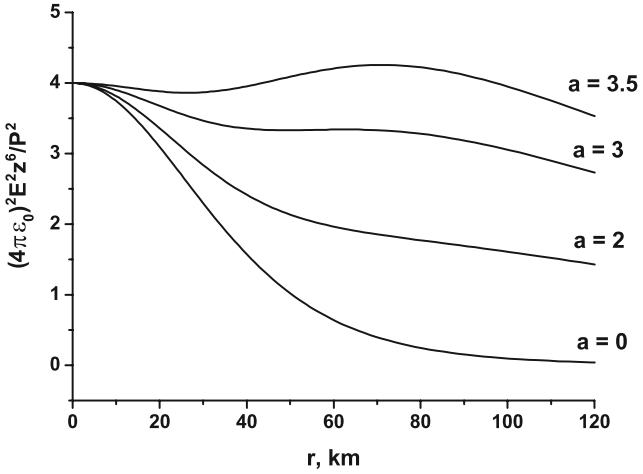


**Figure 4.** Radial distributions of the total electric field (squared, normalized to the magnitude of the dipole field $P/(4\pi\varepsilon_0 z^3)$) at a height of 75 km for different values of parameter *a*.

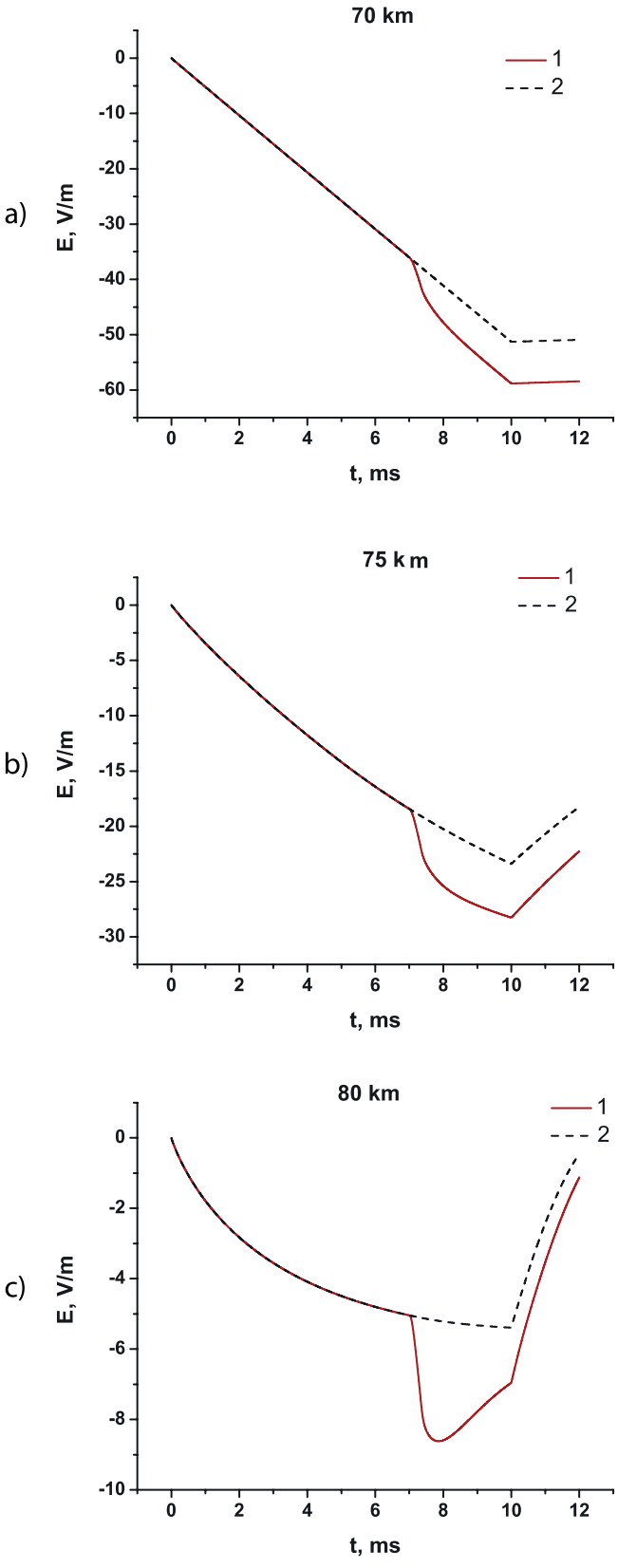


**Figure 5.** Electric field as a function of time at altitudes (a) 70, (b) 75, and (c) 80 km; continuing current magnitude is 10 kA, and M component current peak is 23 kA. Curve 1 is continuing current with M component, and curve 2 is continuing current only.

the microsecond-scale current pulse of the return stroke is neglected in these calculations of the dipole moment for simplicity. M component starts 7 ms after the beginning of the continuing current stage.

[24] The variation of the electric field as a function of time at several altitudes is presented in Figure 5 (for $I$ = 10 kA, $I_0$ = 35 kA, which corresponds to M component current peak of 23 kA) and in Figure 6 (for $I$ = 1 kA, $I_0$ = 3.5 kA). Solid curve corresponds to continuing current with M component and dashed curve to continuing current only. One can see an abrupt increase in the electric field due to the M component and, after 10 ms, the field relaxation with the characteristic decay time decreasing with altitude.

[25] Of interest are the maxima in the field at sufficiently large altitudes which reflect the relation between the relaxation time and characteristic time of M component field growth. At large altitudes, relatively fast increase in current due to M component leads to a considerable field growth, but the latter is soon followed by exponential field relaxation. Figures 5 and 6 illustrate also the role of heating, because for higher currents the heating leads to a decrease in the mean conductivity above the cloud and therefore to more effective field penetration to greater altitudes.

[26] It follows from Figure 5b that because of sufficiently high values of the electric field, the conductivity at the height of 75 km (which is important for sprite initiation) decreases as a result of the electron heating and only slightly influences the electric field. In contrast, for smaller values of current (see Figure 6b) the influence of conductivity is substantial. The growth of electric field at the continuing current stage is saturated. The electric field of the M component does not have enough time for relaxation because of the fast growth of the effective dipole moment, which gives an additional contribution to the field growth: the field increases more than twofold relative to the continuing current stage value. This effect is purely dynamic and cannot be explained in the framework of simple electrostatic approximations. At the end of the M component, the effective dipole moment is almost constant, which leads to the relaxation of the electric field to a stationary value, determined by the background continuing current process. Figure 6c describes similar processes for very small relaxation times, so that the field is saturated rapidly at the continuing current stage, while the occurrence of M component increases the electric field by more than a factor of 7.

[27] The vertical profiles of electric field for three time instances: 7 ms (the time of M component onset), 7.5 ms (approximately the time of effective dipole moment establishment), and 8 ms, are presented in Figures 7 and 8 for two values of maximum M component current and background continuing current (relatively high and relatively low, respectively). These field profiles are to be compared with the critical field for electrical breakdown, which depends on the particular mechanism, with a discussion of possible mechanisms being outside the scope of this paper. However, regardless of the mechanism, critical breakdown field should decrease with altitude in accordance with the neutral gas density $N(z)$. In this paper, for illustrative purposes, we use the following model curves in Figure 7: $8 \times 10^{-15}\,N(z)$, relativistic breakdown field; $1.7 \times 10^{-14}\,N(z)$, minimum field required for propagation of positive streamers; $5 \times 10^{-14}\,N(z)$, minimum field required for

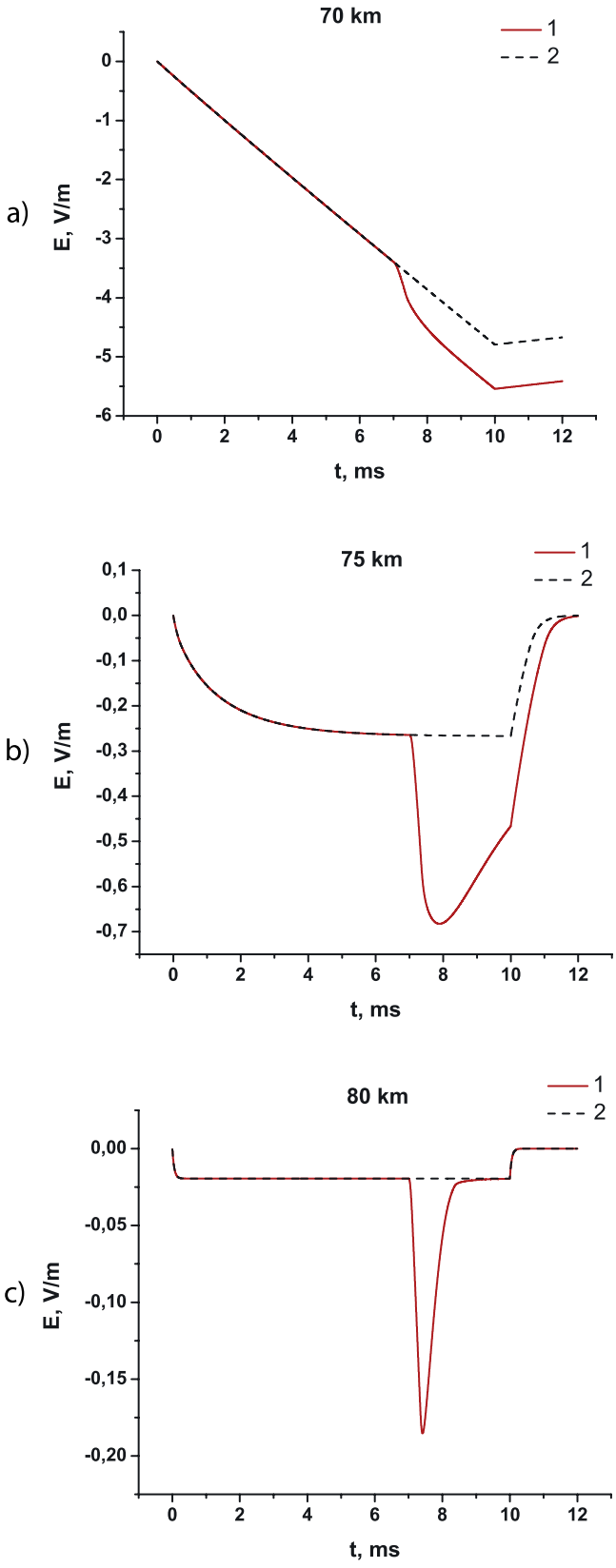


**Figure 6.** Electric field as a function of time at altitudes (a) 70, (b) 75, and (c) 80 km; continuing current magnitude is 1 kA, and M component current peak is 2.3 kA. Curve 1 is continuing current with M component, and curve 2 is continuing current only.

propagation of negative streamers; and $1.2 \times 10^{-13}$ $N(z)$, field at which the ionization rate exceeds attachment rate [see, e.g., *Pasko*, 2006]. Note that the fields are in V/m, if the electron density $N(z)$ is in $cm^{-3}$. It appears that a 23-kA M component (see Figure 7) has a potential to produce electrical breakdown at high altitudes. A 2.3-kA M component (see Figure 8) is unlikely to produce sprites.

## 5. Summary

[28] In spite of significant progress in observations and modeling of transient luminous events (sprites, elves, and sprite halos) in the middle atmosphere, a number of questions remain unanswered and warrant additional research. In particular, a more adequate description of lightning discharge and electric charge distribution in the thundercloud prior to transient luminous events is needed. In the present paper, a simple model is suggested that allows analytical estimations for the electrostatic, induction, and radiation field perturbations above the cloud due to an M component superimposed on continuing current. Various features of spatial distribution of the electric field are examined. In order to take into account the effects of conducting atmosphere on electric fields, numerical calculations have been performed using an experimentally observed night atmosphere conductivity profile. It is found that the field maximum due to transient contribution from M component corresponds to a certain angle, depending on parameter $a = \frac{z^2 \ddot{d}}{Pc^2}$, where $z$ is the altitude, $\ddot{d}$ is the second-order derivative of the dipole moment, $P$ is the full dipole moment of the lightning current, and $c$ is the speed of light in

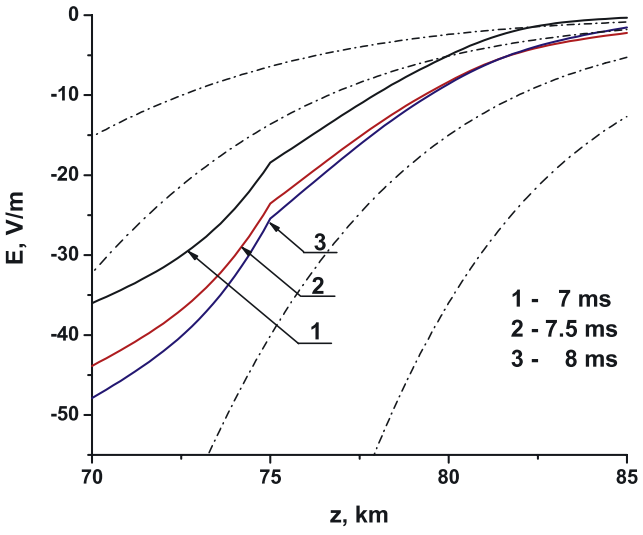


**Figure 7.** Electric field as a function of altitude at time instants, 7, 7.5, and 8 ms; continuing current magnitude is equal to 10 kA, and maximum of M component current is 23 kA. Dash-dotted curves correspond to the critical fields (top to bottom) $8 \times 10^{-15}$ $N(z)$, relativistic breakdown field; $1.7 \times 10^{-14}$ $N(z)$, minimum field required for propagation of positive streamers; $5 \times 10^{-14}$ $N(z)$, minimum field required for propagation of negative streamers; and $1.2 \times 10^{-13} N(z)$, field at which the ionization rate exceeds attachment rate.

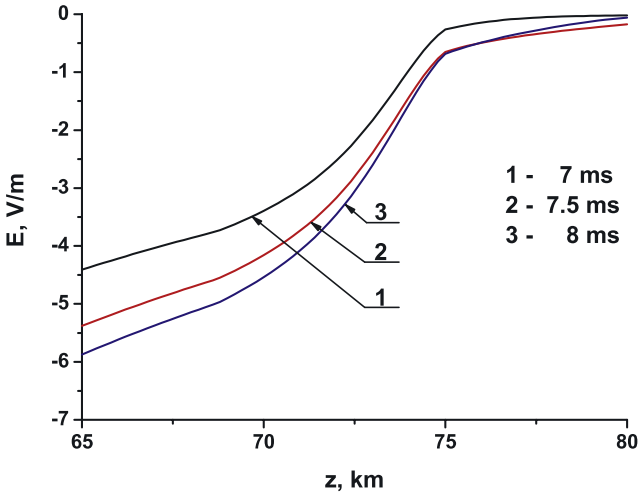


**Figure 8.** Electric field as a function of altitude at time instants, 7, 7.5, and 8 ms; continuing current magnitude is equal to 1 kA, and M component current peak is 2.3 kA.

vacuum. It is concluded that M components have the potential to initiate transient luminous events during the continuing current stage. Since M components follow return strokes after a time interval of a few milliseconds or more, they may be primary producers of so-called delayed sprites. In our opinion, observed features of the spatial and temporal behavior of delayed sprites and sprite halos should be analyzed taking into account lightning M components. In the case of sufficiently small critical fields, M components in negative flashes (that are more numerous than return strokes) can also contribute to excitation of transient luminous events in the middle atmosphere.

## Appendix A: Electron Heating and Its Effect on Conductivity of the Atmosphere

[29] To estimate the change of conductivity due to electron heating in the field, we consider the following expression:

$$\sigma = \frac{e^2 N}{m\nu_e(T_e)}.$$

[30] For estimation of electron heating one can use the equation for the electron temperature $T_e$ written in the form [*Gurevich*, 1978]

$$\frac{dT_e}{dt} = \frac{2}{3}\frac{e^2}{m}\frac{E^2}{\nu_e} - \delta(T_e)\nu_e(T_e)(T - T_e), \tag{A1}$$

where $\delta$ is the fraction of electron energy lost per collision, $\nu_e$ is the frequency of electron collisions, $m$ is the mass of electron, $T$ is the background electron temperature, and the magnetic field is neglected. If the characteristic time of the electric field change is large compared to the time of electron heating $\tau \approx (\delta\nu_e)^{-1}$, equation (A1) is reduced to the corresponding quasi-stationary equation:

$$\left(\frac{E}{E_p}\right)^2 \frac{\nu_e^2(T)\delta(T)}{\nu_e^2(T_e)\delta(T_e)} = \frac{T_e}{T} - 1. \tag{A2}$$

[31] Here $E_p = \sqrt{3\delta(T)\nu_e^2(T)mT/(2e^2)}$ is the characteristic plasma field. It follows from equation (A2) that electrons are weakly heated if $E \ll E_p$, while in the case of $E \gg E_p$ the electron temperature grows substantially. Using the dependence $\delta(T_e)$ and the expression $\nu_e = 1.84 \times 10^9 (N_m/10^{17}\ \mathrm{cm}^{-3})(T_e/10^3\ K)^{\frac{5}{6}}\ s^{-1}$ that is valid for electron temperature of the order of 1 *eV* [*Borisov et al.*, 1986] (where the temperature is measured in $K$ and the air density $N_m$ in $\mathrm{cm}^{-3}$), one can find

$$(E/E_p)^{\frac{3}{4}} = T_e/T, \quad T_e < 10850\ \mathrm{K} \tag{A3}$$

$$(E/E_p)^{\frac{3}{4}} = T_e/T \exp[(T_e - 10850)/6500K], T_e > 10850\ \mathrm{K} \tag{A4}$$

$$\sigma = \sigma(T)\left(\frac{T}{T_e}\right)^{\frac{5}{6}}. \tag{A5}$$

[32] Here, the characteristic temperature values in the argument of the exponential function are obtained from the exponential approximation of known dependence $\delta(T)$ at high temperatures (see *Mareev et al.* [2006] for more details). From the set of equations (A3)–(A5) one can obtain the dependence $\sigma(E)$. The importance of the effect of conductivity perturbation by the field of M component is illustrated in Figure A1. It is seen that the conductivity decreases in the electric field, and this effect becomes more substantial with increasing the altitude (up to 75–80 km) because of the fact that the electric field decreases according to the power law, while the plasma field decreases exponentially. At higher altitudes, this effect diminishes because of the influence of conductivity on the electric field, which because of fast relaxation does not penetrate into the plasma.

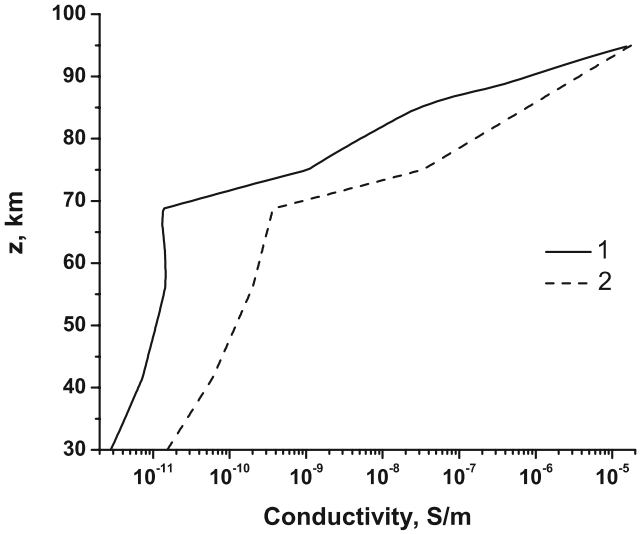


**Figure A1.** Variation of conductivity due to electron heating in the electric field shown in Figure 7 for 8 ms as a function of height. Curve 1 is conductivity profile perturbed by electric field, and curve 2 is conductivity profile in the absence of electric field.

[33] **Acknowledgments.** This work was supported in part by the Russian Foundation for Basic Research (grants 04-02-16634 and 07-02-01342), Russian Academy of Sciences Program "Physics of the Atmosphere: Electric Processes, Radio-Physical Methods, " CRDF grant RUP1-2625-N1-04, and NSF grant ATM-0346164.

## References

Barrington-Leigh, C. P., U. S. Inan, and M. Stanley (2001), Identification of sprites and elves with intensified video and broadband array photometry, *J. Geophys. Res.*, *106*(A2), 1741–1750.

Bell, T. F., S. C. Reising, and U. S. Inan (1998), Intense continuing currents following positive cloud-to-ground lightning associated with red sprites, *Geophys. Res. Lett.*, *25*(8), 1285–1288.

Bering, E. A., III., L. Bhusal, J. R. Benbrook, J. A. Garrett, A. P. Jackson, E. M. Wescott, D. R. Moudry, D. D. Sentman, H. C. Stenbaek-Nielsen, and W. A. Lyons (2004), The results from the 1999 sprites balloon campaign, *Adv. Space Res.*, *34*, 1782–1791.

Borisov, N. D., A. V. Gurevich, and G. M. Milikh (1986), *Artificial Ionization in the Atmosphere* (in Russian), Acad. of Sci., Moscow.

Campos, L. Z. S., M. M. F. Saba, O. Pinto, and M. G. Ballarotti (2007), Waveshapes of continuing currents and properties of M-components in natural negative cloud-to-ground lightning from high-speed video observations, *Atmos. Res*, in press.

Cummer, S. A., and M. Füllekrug (2001), Unusually intense continuing current in lightning produces delayed mesospheric breakdown, *Geophys. Res. Lett.*, *28*(3), 495–498.

Cummer, S. A., U. S. Inan, T. F. Bell, and C. P. Barrington-Leigh (1998), ELF radiation produced by electrical currents in sprites, *Geophys. Res. Lett.*, *25*(8), 1281–1284.

Fisher, R. J., G. H. Schnetzer, R. Thottappillil, V. A. Rakov, M. A. Uman, and J. D. Goldberg (1993), Parameters of triggered lightning flashes in Florida and Alabama, *J. Geophys. Res.*, *98*(D12), 22,887–22,902.

Füllekrug, M., D. R. Moudry, G. Dawes, and D. D. Sentman (2001), Mesospheric sprite current triangulation, *J. Geophys. Res.*, *106*(D17), 20,189–20,194.

Gurevich, A. V. (1978), *Nonlinear Phenomena in the Ionosphere*, Springer, New York.

Holzworth, R. H., M. C. Kelley, C. L. Siefring, L. C. Hale, and J. D. Mitchell (1985), Electrical measurements in the atmosphere and ionosphere over an active thunderstorm: 2. Direct current electric fields and conductivity, *J. Geophys. Res.*, *90*(A10), 9824–9830.

Jacobson, E. A., and E. P. Krider (1976), Electrostatic field changes produced by Florida lightning, *J. Atmos. Sci.*, *33*(1), 103–117.

Lu, G. (2006), Transient electric field at high altitudes due to lightning: Possible role of induction field in the formation of elves, *J. Geophys. Res.*, *111*, D02103, doi:10.1029/2005JD005781.

Mareev, E. A., A. A. Evtushenko, and S. A. Yashunin (2006), On the modeling of sprites and sprite-producing clouds in the global electric circuit, in *Sprites, Elves, and Intense Lightning Discharges*, edited by M. Füllekrug et al., pp. 313–340, Springer, New York.

Pasko, V. P. (2006), Theoretical modeling of sprites and jets, in *Sprites, Elves, and Intense Lightning Discharges*, edited by M. Füllekrug et al., pp. 253–311, Springer, New York.

Pasko, V. P., U. S. Inan, T. F. Bell, and Y. N. Taranenko (1997), Sprites produced by quasi-electrostatic heating and ionization in the lower ionosphere, *J. Geophys. Res.*, *102*(A3), 4529–4561.

Rakov, V. A. (2003), A review of positive and bipolar lightning discharges, *Bull. Am. Meteorol. Soc.*, *84*, 767–776.

Rakov, V. A., and M. A. Uman (2003), *Lightning: Physics and Effects*, 687 pp., Cambridge Univ. Press, New York.

Rakov, V. A., R. Thottappillil, M. A. Uman, and P. P. Barker (1995), Mechanism of the lightning M component, *J. Geophys. Res.*, *100*(D12), 25,701–25,710.

Rakov, V. A., D. E. Crawford, K. J. Rambo, G. H. Schnetzer, M. A. Uman, and R. Thottappillil (2001), M-component mode of charge transfer to ground in lightning discharges, *J. Geophys. Res.*, *106*(D19), 22,817–22,831.

Reising, S. C., U. S. Inan, and T. F. Bell (1999), ELF sferic energy as a proxy indicator for sprite occurrence, *Geophys. Res. Lett.*, *26*(7), 987–990.

Wescott, E. M., H. C. Stenbaek-Nielsen, D. D. Sentman, M. J. Heavner, D. R. Moudry, and F. T. Sao Sabbas (2001), Triangulation of sprites, associated halos and their possible relation to causative lightning and micrometeors, *J. Geophys. Res.*, *106*(A6), 10,467–10,478.

E. A. Mareev and S. A. Yashunin, Laboratory of Geophysical Electrodynamics, Institute of Applied Physics, Russian Academy of Sciences, 46 Ulyanov Street, Nihzny Novgorod 603600, Russia. (mareev@appl.sci-nnov.ru)

V. A. Rakov, Department of Electrical and Computer Engineering, University of Florida, P.O. Box 116130, Gainesville, FL 32611-6130, USA. (rakov@ece.ufl.edu)